Diagn Interv Radiol 2011; 17:297–307

ORIGINAL ARTICLE

Accuracy of parathyroid imaging: a comparison of planar scintigraphy, SPECT, SPECT-CT, and C-11 methionine PET for the detection of parathyroid adenomas and glandular hyperplasia

Mehmet Özer Öksüz, Helmut Dittmann, Corinna Wicke, Karsten Müssig, Roland Bares, Christina Pfannenberg, Susanne Martina Eschmann

PURPOSE
To compare the accuracy of planar scintigraphy, single photon emission computed tomography (SPECT), SPECT-CT, and positron emission tomography (PET) with C-11 methionine for the pre-operative detection of parathyroid adenomas.

MATERIALS AND METHODS
We retrospectively evaluated the pre-operative studies of 60 patients with primary (n=56) and secondary (n=4) hyperparathyroidism. In 25/60 patients (Group 1), only planar scans were obtained, and additional SPECT and SPECT-CT were carried out in 35/60 patients (Group 2). PET or PET-CT with C-11 methionine was conducted in 8/60 patients (Group 3).

RESULTS
The results of the planar scans (Group 1) were true positive in 19/25 patients and false negative in 6/25 patients (sensitivity per patient, 76%). Histopathology confirmed 27 adenomas and two hyperplasia. Planar imaging identified 20/29 of these pathologies, whereas 9/29 were missed (sensitivity per adenoma, 69%). SPECT (Group 2) results were true positive in 34/35 patients and false negative in only one case (sensitivity per patient, 97%). On a lesion-based analysis, 38 adenomas were identified, and two were missed (sensitivity per adenoma, 95%). The sensitivities of SPECT and SPECT-CT were equal; however, SPECT-CT provided superior topographic information. C-11 methionine PET (Group 3) results were true positive in all eight patients. In one case, surgery confirmed two ipsilateral adenomas, only one of which was identified by PET (sensitivity per patient, 100%; per adenoma, 88.9%).

CONCLUSION
SPECT is superior to planar imaging. SPECT-CT has identical sensitivity compared to SPECT alone, but it provides additional topographic information. The sensitivity of PET appears to be even higher compared to SPECT. In the case of negative scintigraphic findings and proven hyperparathyroidism, additional C-11 methionine PET or PET-CT is recommended.

Key words: • hyperparathyroidism • scintigraphy • SPECT • C-11 methionine • PET scan

From the Department of Radiology and Nuclear Medicine (M.Ö.Ö. ✉ *oeksuezm@uhbs.ch*), Basel University Hospital, Basel, Switzerland; the Departments of Nuclear Medicine (H.D., R.B.), General, Visceral, and Transplant Surgery (C.W.), Internal Medicine, Division of Endocrinology, Diabetology, Nephrology, Angiology, and Clinical Chemistry (K.M.), and Radiology, (C.P.),Tübingen University Hospital, Tübingen, Germany; and the Department of Nuclear Medicine (S.M.E.), Marienhospital Stuttgart, Teaching Hospital of Tübingen University Hospital, Stuttgart, Germany.

Received 31 March 2010; revision requested 11 July 2010; revision received 8 August 2010; accepted 10 December 2010.

Published online 8 February 2011
DOI 10.4261/1305-3825.DIR.3486-10.1

Sporadic primary hyperparathyroidism is the most common cause of hypercalcemia in the outpatient population, with a prevalence of one per 500 women and one per 2000 men over 40 years of age. Both increased cell proliferative activity and a decreased sensitivity of cells to secretory inhibition by calcium occur in hyperparathyroidism (1). The diagnosis of hyperparathyroidism is usually made by the demonstration of an inappropriately elevated parathyroid hormone level compared to the simultaneously measured serum calcium level (2). In 80% to 85% of patients, primary hyperparathyroidism is caused by one or more parathyroid adenomas, and in 15% to 20% of cases, it is the result of parathyroid hyperplasia. A rare cause of primary hyperparathyroidism, accounting for less than 1% of all cases, is parathyroid carcinoma. Persistent hyperparathyroidism occurs in 5% to 10% of all patients who undergo surgery for primary hyperparathyroidism, with a continuation of the pre-operative hypercalcemia in the immediate post-operative period. Hyperparathyroidism that presents after a period of more than six months of normocalcemia following surgery is called "recurrent hyperparathyroidism" and is commonly due to continuing growth of the remaining parathyroid glands (3). Secondary hyperparathyroidism is a compensatory hypertrophy of all parathyroid glands due to hypocalcemia, as occurs in renal failure or with vitamin D deficiency (4), whereas tertiary hyperparathyroidism describes the development of autonomous function of parathyroid tissue after longstanding secondary hyperparathyroidism (5–8).

In most cases (80%–85%), parathyroid adenomas are found adjacent to the thyroid gland, which is the normal location for these adenomas. However, in up to 20% of cases, they are ectopically placed, e.g., in the anterosuperior, posterosuperior, or very rarely in the mid-lower mediastinum. Occasionally, parathyroid adenomas may be found within, or lateral to, the carotid sheath. Rarely, the lower parathyroid glands fail to migrate, remaining in the high neck anterior to the carotid bifurcation. Finally, 1.4% to 3.2% of all parathyroid adenomas are intrathyroidal, i.e., embedded completely within the thyroid gland (9).

Among the several imaging procedures that have been developed for the detection and localization of parathyroid adenomas, dual-phase scintigraphy with Tc-99m sestamibi combined with ultrasonography is considered the imaging method of choice for pre-operatively localizing parathyroid adenomas. The overall accuracy of dual-phase scintigraphy combined with ultrasonography has been found to be superior to that of other scintigraphic or radiological techniques (10, 11). Studies comparing planar imaging and single photon emission computed tomography (SPECT) have shown significantly increased sensitivity for Tc-99m sestamibi SPECT, thus supporting its routine use prior to surgery (12–14).

In this study, we compared the accuracies of planar scintigraphy, SPECT, SPECT-CT with Tc-99m sestamibi and positron emission tomography (PET) with C-11 methionine for the detection of parathyroid adenomas and/or hyperplasia.

Materials and methods

Patients

A total of 60 patients (44 females, 16 males) with a mean age of 51±29 years (range, 22–80 years) with biochemical evidence of hyperparathyroidism, i.e., increased serum calcium and parathyroid hormone concentrations, that were scheduled for surgery were evaluated. Fifty-six patients had primary hyperparathyroidism, and four had secondary hyperparathyroidism. One case of primary hyperparathyroidism was associated with multiple endocrine neoplasia type 1 (MEN 1).

All patients underwent ultrasound of the neck and parathyroid scintigraphy with Tc-99m sestamibi. Patients with concomitant thyroid disease received an additional thyroid scan with Tc-99m pertechnetate.

In 25 patients, only planar scans with Tc-99m sestamibi were obtained (Group 1) (Table 1). In 35 patients, additional SPECT and SPECT-CT was carried out (Group 2) (Table 1). PET (4 patients) or PET-CT (4 patients) with C-11 methionine was performed in 8 of the 60 patients (Group 3) (Table 1).

The local ethics committee approved the study, and written informed consent was obtained from all patients before they were enrolled in the study.

Ultrasonography

In all patients, a pre-operative high-resolution ultrasound of the thyroid gland and surrounding tissues was performed with 7.5- to 10-MHz transducers. Parathyroid adenomas were identified as hypoechoic nodules with well-defined margins that were mostly localized outside the thyroid gland.

Planar scintigraphy

Anterior planar views of the neck and thorax (10 min/frame; matrix size, 256×256) were acquired with the patients in the supine position. Images were obtained at 10 min (thyroid phase) and 120–150 min (parathyroid phase) after intravenous injection of 400 MBq (10.81 mCi) Tc-99m sestamibi using a large field-of-view gamma camera equipped with a high-resolution collimator.

SPECT and SPECT-CT

SPECT-CT imaging of the neck and thorax was carried out immediately after the planar imaging using a dual-head variable-angle gamma camera with a low-power X-ray CT transmission system mounted on the same gantry (Millennium VG Hawkeye, GE Medical Systems, Carrollton, Texas, USA). The transmission data were reconstructed using filtered back-projection to produce cross-sectional attenuation images in which each pixel represents the estimated X-ray attenuation of the imaged tissue. The SPECT component of the study was then obtained in 120 projections, with a 3° angle step, in a 128×128 matrix, and at 20 s per view. Reconstruction was performed iteratively using the ordered subsets expectation maximization technique (OSEM). The emission images, obtained in transaxial, sagittal, and coronal planes, were inherently registered to the anatomic maps using eNTEGRA workstation software (GE Medical Systems) followed by the generation of hybrid images of the superimposed transmission (CT) and emission (SPECT) data.

Table 1. Pre-operative studies of 60 patients with primary hyperparathyroidism (n=56) and secondary hyperparathyroidism (n=4)

Group	Imaging technique	Number of patients	Concomitant thyroid disease
1	Planar	25	7
2	SPECT and SPECT-CT	35	9
3	PET and PET-CT[a]	8	3

For 25 patients (Group 1), only planar scans were obtained, and in 35 patients (Group 2), additional SPECT and SPECT-CT was carried out.
[a]PET or PET-CT with C-11 methionine was carried out in 8 patients (Group 3, 4x PET and 4x PET-CT).

Thyroid scintigraphy

Seven patients in Group 1 and nine patients in Group 2 with concomitant thyroid nodules also obtained a planar thyroid scan following the administration of 75 MBq (2.03 mCi) of Tc-99m pertechnetate for comparison with earlier parathyroid images.

PET and PET-CT

In four patients, PET was performed with a dedicated PET scanner (Advance, GE Medical Systems, Milwaukee, Wisconsin, USA). Fifteen minutes after the intravenous injection of 700 MBq (18.92 mCi) of C-11 methionine, two contiguous 15-min emission scans were performed of the neck and upper mediastinum followed by two 10-min transmission scans for the attenuation correction using a Ge-68 source.

Four patients underwent imaging with a dedicated PET-CT system (Biograph 16 HiRez, Siemens Medical Solutions, Erlangen, Germany) 15 min after the intravenous injection of 700 MBq (18.92 mCi) of C-11 methionine. Images of the neck and thorax, from the base of the skull to the diaphragm, were obtained in three consecutive bed positions, each of which was 5 min in duration. For attenuation correction, a non-contrast CT scan was performed first and was followed by a contrast-enhanced CT protocol (Ultravist 370, Schering, Berlin, Germany).

Image interpretation

The datasets of planar scintigraphy, SPECT and SPECT-CT, PET and PET-CT were interpreted visually by a team of three nuclear medicine physicians and two radiologists. In cases of questionable findings, the decision was made by consensus of at least two observers. A distinct focus of increased uptake within or neighboring the thyroid in the mediastinum on either an early or a late image, or both, was considered positive for abnormal parathyroid tissue, unless it could be attributed to a thyroid nodule using the pertechnetate scan. The SPECT-CT and PET-CT images were analyzed for adenoma localization in relation to adjacent anatomic structures. The final diagnosis of a parathyroid adenoma, whether cervical or ectopic, was based on the intraoperative and pathologic findings.

Data analysis

Planar scintigraphy, SPECT and SPECT-CT studies for all patients; PET studies for four patients; and PET-CT studies for four patients were retrospectively analyzed. This was followed by an assessment of the detectability rate and the sensitivity of these modalities, as defined by surgical findings and histopathologic confirmation. SPECT or SPECT-CT was considered to be helpful in image interpretation if it provided precise localization with respect to the depth of the suspected lesion and its relation to adjacent structures including the thyroid gland, trachea, esophagus, thymus, spine, and sternum. The chi-square test and the Wilcoxon test were used for statistical analysis of the sensitivities.

Surgery and histopathology

All patients underwent surgical exploration. The appearance, size, and location of every parathyroid gland were documented. Histopathologic examination was performed, and weights and volumes of all resected specimens were obtained.

Results

Parathyroidectomy was performed in all 60 patients after parathyroid imaging revealed 63 parathyroid adenomas and six hyperplastic parathyroid glands.

Group 1 (planar imaging)

The results of the planar scans were true-positive in 19/25 patients and false-negative in 6/25 patients. Histopathology confirmed 27 adenomas and two cases of hyperplasia, i.e., one patient with secondary hyperparathyroidism and one patient with MEN 1 who had a hyperplastic parathyroid gland and a contralateral adenoma. Twenty adenomas and two hyperplastic parathyroid glands were identified by planar imaging, whereas nine adenomas were missed. This leads to a sensitivity per patient of 76% and per adenoma of 69% (Table 2). In two patients, only one of two adenomas was detected. In both cases, the contralateral smaller-sized adenoma was missed. In three patients, the detected adenomas were placed ectopically in the anterosuperior mediastinum (Table 3).

Group 2 (SPECT and SPECT-CT)

The SPECT images were true-positive in 34/35 patients (Fig. 1) and false-negative in only one case. In one patient, only one of two adenomas was identified. In another patient, SPECT images revealed two foci, whereas surgery and histopathology confirmed only one adenoma and a contralateral thyroid nodule. The lesion-based analysis revealed that 38 adenomas were identified with SPECT, and only two parathyroid adenomas were missed. In four cases, histology revealed hyperplastic parathyroids, and all were true-positives. This leads to a sensitivity per patient of 97% and per adenoma of 95% (Table 2).

In five patients, six abnormal parathyroid glands were found in ectopic locations. One patient had one adenoma and one hyperplastic parathyroid gland in the anterosuperior mediastinum. Another patient had one adenoma in the anterosuperior mediastinum and one adenoma in an anatomically correct position, i.e., posterior to the lower pole of the right thyroid lobe. In one case, the adenoma was located in the mid-lower mediastinum in proximity to the left main bronchus (Figs. 2 and 3), and in the next patient, the parathyroid adenoma was located in the posterosuperior mediastinum near the aortic arch/descending aorta. Finally, in one patient, the atypical adenoma was embedded within the lower pole of the left thyroid gland, i.e., an intrathyroidal parathyroid adenoma (Table 3).

The sensitivities of SPECT and SPECT-CT were equal. However, SPECT-CT provided superior topographic information, particularly in those patients with ectopic localization of parathyroid adenomas (Fig. 3).

Group 3 (PET and PET-CT)

C-11 methionine-PET images were true-positive in all eight patients (Fig. 4). In one case, surgery confirmed two ipsilateral adenomas, only one of which was identified by PET (sensitivity per patient of 100% and per adenoma of 88.9%).

In Group 1 (planar imaging) and Group 2 (SPECT and SPECT-CT), the size of the parathyroid glands showed a wide range from relatively small to fairly large volumes of 0.01 mL up to 4.41 mL (Fig. 5, Tables 4 and 5). Adenomas that were missed were generally smaller than the majority of all parathyroid adenomas (statistically significant in Group 1 with [P = 0.014] and without [P = 0.027] the two large true-positive adenomas based on the Wilcoxon test).

Table 2. Patient- and lesion-based sensitivities of Group 1 (planar scintigraphy) and Group 2 (SPECT and SPECT-CT) using the chi-square test

Group	Patient-based sensitivity	Lesion-based sensitivity
1	76%	69%
2	97%	95%
	P = 0.017	P = 0.005

Table 3. Ectopic adenomas in Group 1 (planar imaging) and Group 2 (SPECT and SPECT-CT)

Group	Patients	Pathology	Localization
1	3	1 adenoma in each patient	Anterosuperior mediastinum
2	1	1 adenoma and 1 case of hyperplasia	Anterosuperior mediastinum
	1	2 adenomas	Eutopic (1x) and anterosuperior mediastinum (1x)
	1	1 adenoma	Mid-lower mediastinum
	1	1 adenoma	Posterosuperior mediastinum
	1	1 adenoma	Intrathyroidal

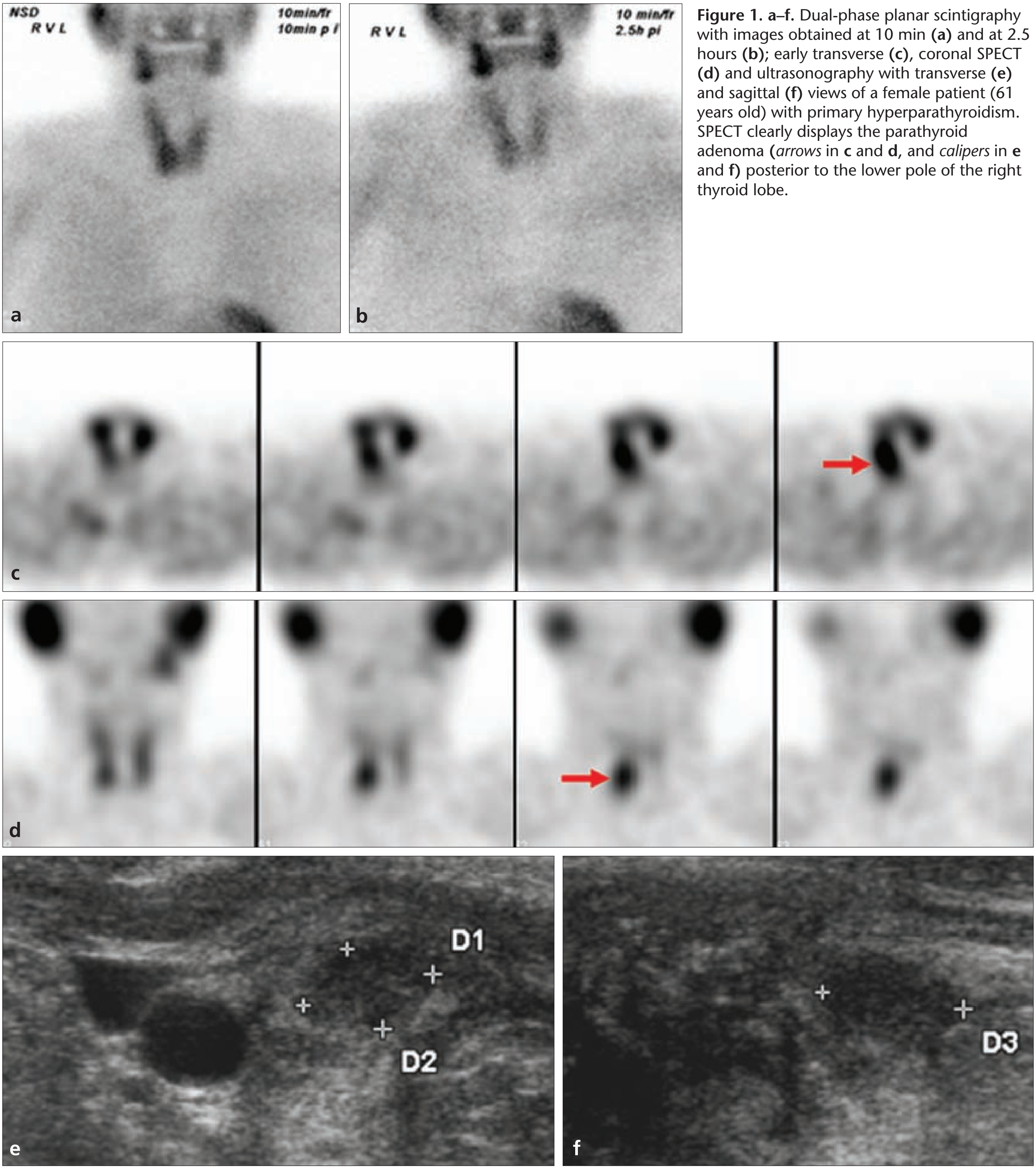

Figure 1. a–f. Dual-phase planar scintigraphy with images obtained at 10 min **(a)** and at 2.5 hours **(b)**; early transverse **(c)**, coronal SPECT **(d)** and ultrasonography with transverse **(e)** and sagittal **(f)** views of a female patient (61 years old) with primary hyperparathyroidism. SPECT clearly displays the parathyroid adenoma (*arrows* in **c** and **d**, and *calipers* in **e** and **f)** posterior to the lower pole of the right thyroid lobe.

Discussion

Contemporary modalities that help endocrine surgeons localize abnormal parathyroid glands in patients with hyperparathyroidism provide high-resolution anatomical and functional images of hyperactive endocrine tissue. When used in tandem, neck ultrasound and Tc-99m sestamibi parathyroid scintigraphy using various imaging techniques (subtraction or dual-phase imaging) have been shown to be effective in localizing adenomas to allow pre-operative planning and intra-operative decision making (15–20).

Focused neck exploration in patients with primary hyperparathyroidism has recently replaced the traditional bilateral approach due to a decrease in operative morbidity and a shortening

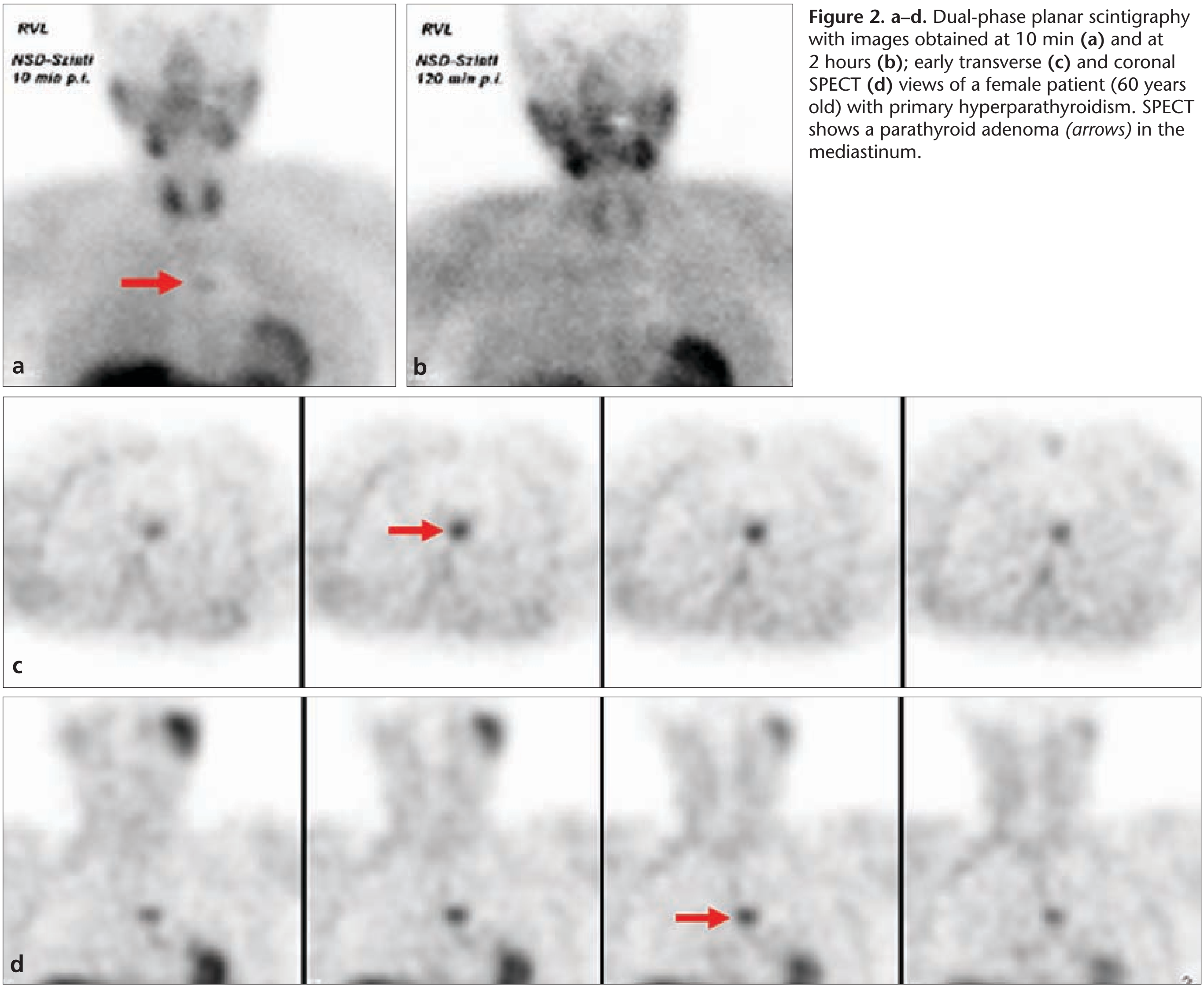

Figure 2. a–d. Dual-phase planar scintigraphy with images obtained at 10 min **(a)** and at 2 hours **(b)**; early transverse **(c)** and coronal SPECT **(d)** views of a female patient (60 years old) with primary hyperparathyroidism. SPECT shows a parathyroid adenoma *(arrows)* in the mediastinum.

of hospitalization time. However, the limited surgical procedures require optimal pre-operative localization studies (21, 22).

Planar scintigraphy has been considered the primary imaging modality for the pre-operative localization of parathyroid adenomas with pooled sensitivities of 87% for subtraction imaging and 73% for dual-phase imaging (23). The results of the present study (Group 1) revealed sensitivities of 76% on patient-based and 69% on lesion-based analysis and are within the range of the results from the dual-phase methods reported in the literature (24).

Our study comparing planar imaging and SPECT supports the wide application of SPECT, which has increased sensitivities compared to planar scintigraphy of 97% on patient-based and 95% on lesion-based analysis. These values are similar to previously published data with sensitivities ranging from 92% to 96 % (25–29).

In the present study, the patient- and lesion-based sensitivities of SPECT and SPECT-CT were equal for the detection rate of parathyroid adenomas. However, SPECT-CT provided superior topographic information, particularly in those patients with an ectopic localization of parathyroid adenomas, facilitating a surgical approach by providing anatomic mapping prior to exploration (30).

Gland volume (weight) and gland vascularity are known to have an influence on radionuclide uptake. They probably correlate with an increased delivery and, consequently, with an increased accumulation of radiotracer in an abnormal parathyroid gland (31). Planar imaging (Group 1) identified 20/29 parathyroid adenomas (69%) with volumes ranging from 0.29 mL to 3.91 mL but missed 9/29 adenomas with gland volumes of 0.16 mL to 1.2 mL, whereas SPECT and SPECT-CT (Group 2) were able to detect 38/40 adenomas (95%) with volumes between 0.01 mL and 4.41 mL (Fig. 5). Two small adenomas (0.3 and 0.36 mL) were missed. These findings illustrate that the increased sensitivity of SPECT and SPECT-CT compared to planar scintigraphy can be attributed to a higher detection rate of particularly small adenomas due to a superior contrast resolution, depth information and accurate three-dimensional localization.

Histopathology of the two false-negative findings of Group 2 (SPECT

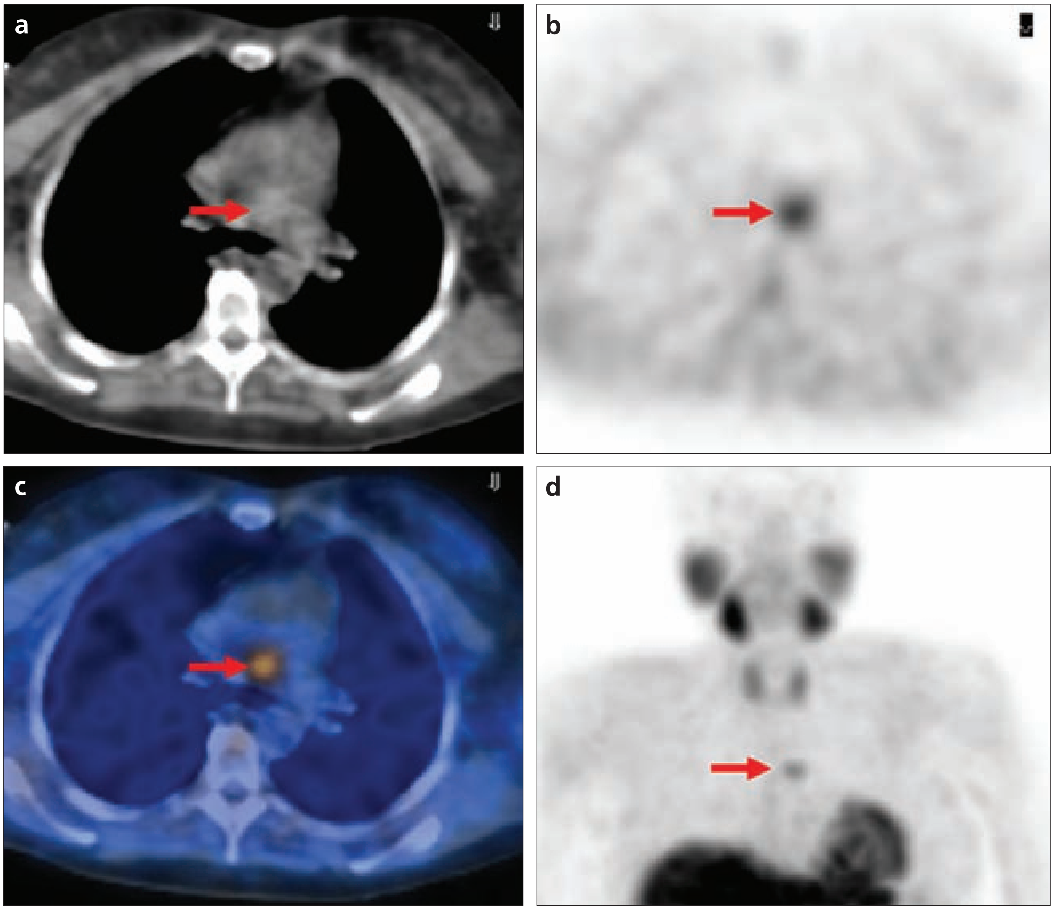

Figure 3. a–d. Low-dose CT **(a)**, transverse SPECT **(b)**, fusion of low-dose CT and SPECT **(c)**, and three-dimensional maximum intensity projection **(d)**. SPECT-CT of the same patient as in Figure 2 provides additional topographic information by depicting neighboring anatomical structures. The parathyroid adenoma *(arrows)* is located in the mid-lower mediastinum in the proximity of the left main bronchus.

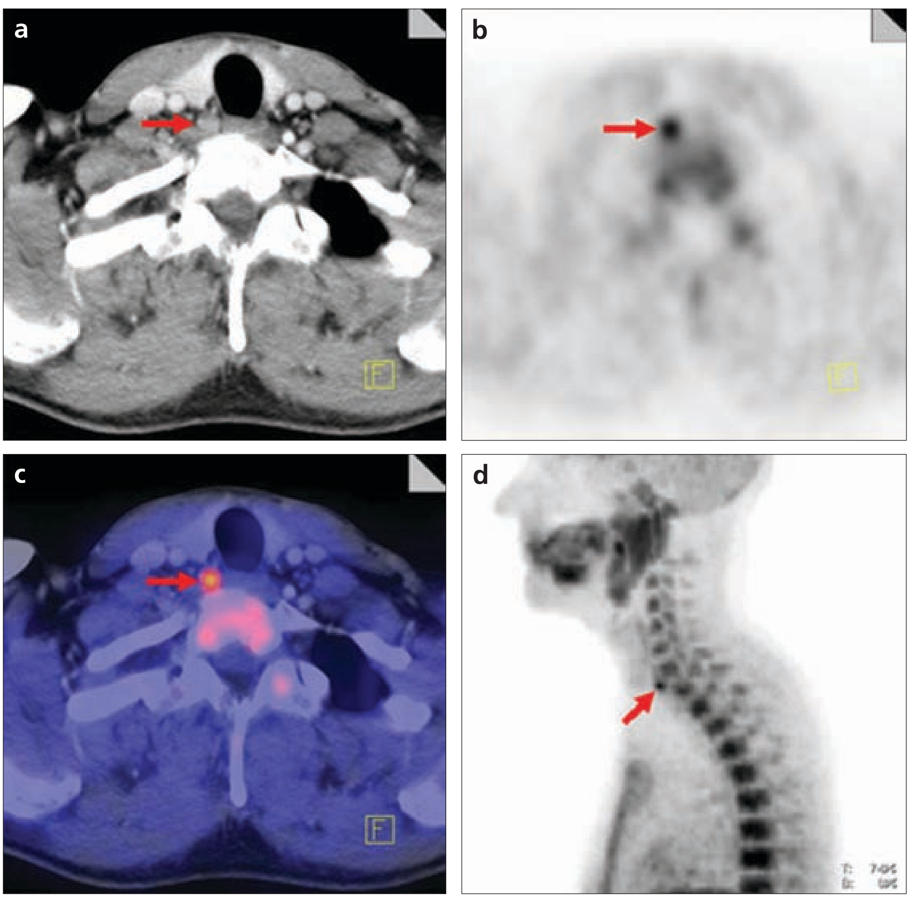

Figure 4. a–d. Contrast-enhanced CT **(a)**, transverse PET **(b)**, fusion of contrast-enhanced CT, and PET **(c)** and sagittal three-dimensional maximum intensity projection **(d)** of a 47-year-old male patient with primary hyperparathyroidism. C-11 methionine PET-CT reveals a small parathyroid adenoma *(arrows)* posterior to the lower pole of the right thyroid lobe.

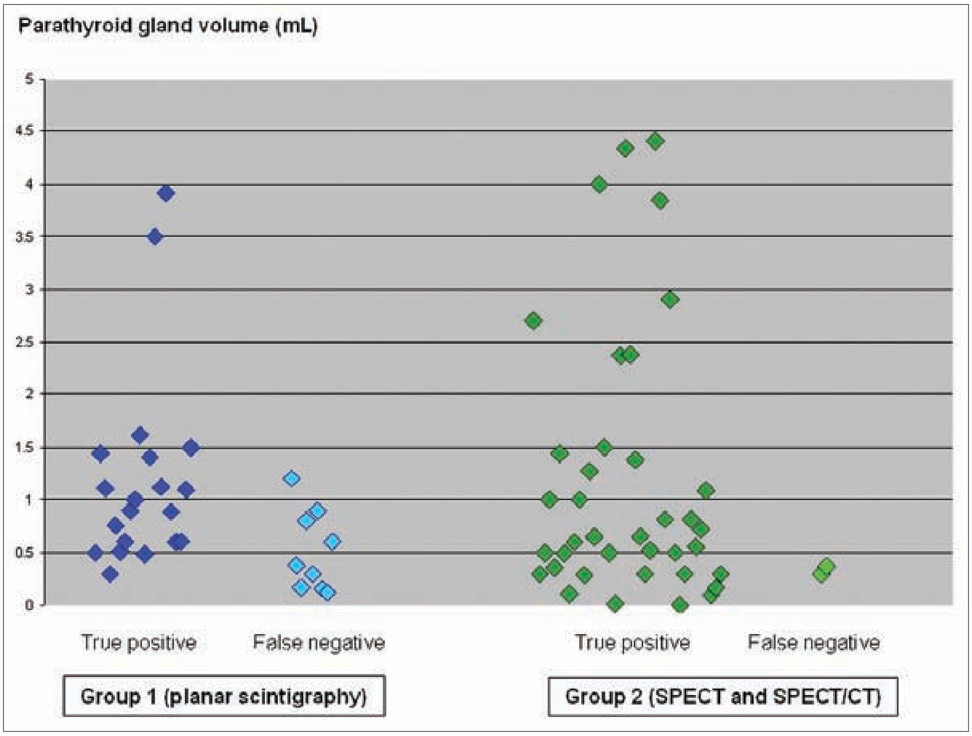

Figure 5. Gland volumes of detected (true positive) and non-detected (false negative) enlarged parathyroid glands (adenoma, hyperplastic gland). The increased sensitivity of SPECT and SPECT-CT (Group 2) compared to planar scintigraphy (Group 1) can be attributed to a higher detection rate of particularly small adenomas due to a superior contrast resolution, depth information and accurate three-dimensional localization.

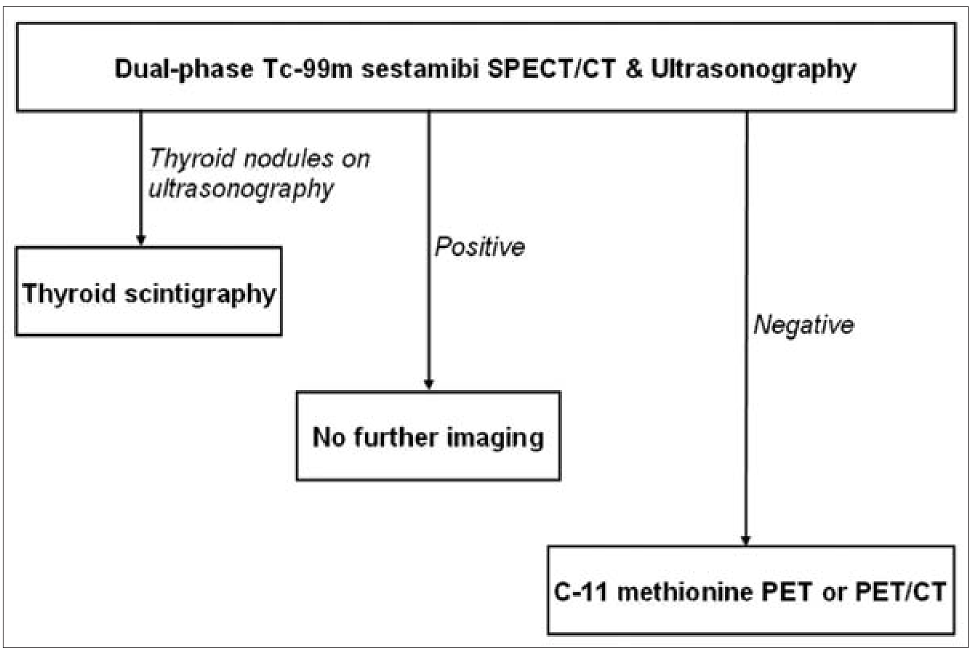

Figure 6. Imaging algorithm for patients with proven hyperparathyroidism. Dual-phase Tc-99m sestamibi SPECT-CT in combination with ultrasonography imaging is the method of choice to localize parathyroid adenomas and/or hyperplasia. If thyroid nodules are found on ultrasonography, thyroid scintigraphy should be performed. In the case of negative scintigraphic findings, C-11 methionine PET or PET-CT should be performed.

and SPECT-CT) revealed that one of the missed adenomas was characterized by only a few adenoma-like cells corresponding to a low functional status. In the other case, one of two adenomas was correctly depicted, but the missed adenoma showed a fairly low content of oxyphil cells. As previously reported, the presence of oxyphil cells that are rich in mitochondria is essential for radionuclide retention (32).

It has been reported in the literature that parathyroid scintigraphy with Tc-99m sestamibi is less sensitive in the detection of hyperplastic parathyroid glands compared to parathyroid adenomas (33, 34). However, in our study, all false-negative cases occurred in patients with primary hyperparathyroidism with histopathologically small parathyroid adenomas. The six hyperplastic parathyroid glands, two in Group 1 (secondary hyperparathyroidism, MEN 1) and four in Group 2 (secondary hyperparathyroidism in three cases, primary hyperparathyroidism in one case) were correctly detected.

Although 80% to 85% of parathyroid adenomas are found adjacent to the thyroid gland in their normal position, up to 20% are located at ectopic sites. The term "major ectopy" refers to parathyroid adenomas located in the mediastinum; high in the neck,

Table 4. Comparison of pre-operative scintigraphy and post-operative pathology of Group 1 (planar scintigraphy) with volumes of parathyroid adenomas/hyperplasias

Pre-operative diagnosis	Pre-operative scintigraphy	Post-operative pathology	Scintigraphy vs. pathology	Volume (mL)
pHPT	Right inferior	PA right inferior	TP	0.5
pHPT	Right inferior	PA right inferior	TP	1.44
sHPT	Left superior	PH left superior	TP	1.11
pHPT	Right inferior	PA right inferior	TP	0.29
pHPT	Anterosuperior mediastinum	PA anterosuperior mediastinum	TP	0.75
pHPT	Right superior	PA right superior	TP	0.51
pHPT	Anterosuperior mediastinum	PA anterosuperior mediastinum	TP	0.6
pHPT	Left inferior	PA left inferior	TP	0.9
pHPT	Left inferior	PA left inferior	TP	1.0
pHPT	Right inferior	PA right inferior	TP	1.62
pHPT	Right superior	PA right superior	TP	0.48
pHPT	Right inferior	PA right inferior	TP	1.4
pHPT	Left superior	PA left superior	TP	3.5
pHPT	Left superior	PA left superior	TP	1.12
pHPT	Anterosuperior mediastinum	PA anterosuperior mediastinum	TP	3.91
pHPT (MEN 1)	Right superior, left inferior	PA right superior, PH left inferior	TP (2x)	0.6, 0.88
pHPT	Left inferior	PA left inferior	TP	0.6
pHPT	None	PA right superior	FN	1.2
pHPT	None	PA right inferior, PA left superior	FN (2x)	0.16, 0.38
pHPT	None	PA left inferior	FN	0.8
pHPT	Right inferior	PA right inferior, PA left inferior	TP (right), FN (left)	1.1, 0.3
pHPT	Right inferior	PA right inferior, PA left superior	TP (right), FN (left)	1.5, 0.9
pHPT	None	PA right inferior	FN	0.15
pHPT	None	PA left inferior	FN	0.12
pHPT	None	PA right inferior	FN	0.6

pHPT, primary hyperparathyroidism; sHPT, secondary hyperparathyroidism; MEN, multiple endocrine neoplasia; PA, parathyroid adenoma; PH, parathyroid hyperplasia; TP, true positive; FN, false negative.

in, or lateral to, the cervical neurovascular bundle; or within the thyroid gland (35). In our study, we found ectopic adenomas in 9 out of 60 patients (15%), which is comparable to figures reported in the literature (8% to 20%) (36–38). Most of the ectopic adenomas (6/9) were localized in the anterior superior mediastinum. One patient had an ectopically located parathyroid adenoma in the mid-lower mediastinum on the ventral aspect of the left main bronchus (Figs. 2 and 3), and in another patient, the parathyroid adenoma was located in the posterior superior mediastinum near the aortic arch/descending aorta.

As a rare cause of primary hyperparathyroidism, we found an intrathyroidal parathyroid adenoma within the lower pole of the thyroid gland. Based on the known embryology, it was originally thought that intrathyroidal adenomas would involve only the superior parathyroid glands (39, 40). However, data available from more recent reviews have shown that intrathyroidal parathyroid adenomas or hyperplastic glands may involve either the superior or inferior glands (41–43).

One patient in our study had two anomalous parathyroid glands, i.e., one adenoma and one hyperplastic parathyroid gland, and both were ectopically located in the anterior superior mediastinum. Current evidence regarding the histopathogenesis of parathyroid adenoma and hyperplasia is unclear. Although most adenomas are monoclonal proliferations, suggesting a neoplastic origin, histopathologic evidence indicates the evolution to a monoclonal adenoma from polyclonal hyperplasia and vice versa (44–46). Therefore, parathyroid adenoma and hyperplasia could be the same disease entity, representing opposite ends of the spectrum of phenotypic expression. The prevalence of hyperplasia varies considerably in different studies, and there appears to be a strong influ-

Table 5. Comparison of pre-operative scintigraphy and post-operative pathology of Group 2 (SPECT and SPECT-CT) with volumes of parathyroid adenomas/hyperplasias

Pre-operative diagnosis	Pre-operative scintigraphy	Post-operative pathology	Scintigraphy vs. pathology	Volume (mL)
sHPT	Right inferior, left superior, left inferior	PA right inferior, PA left superior, PH left inferior	TP (3x)	0.5, 2.7, 0.29
sHPT	Anterosuperior mediastinum (2x)	PA (1x) and PH (1x) anterosuperior mediastinum	TP (2x)	0.35, 1.0
pHPT	Right inferior	PA right inferior	TP	1.44
sHPT	Left inferior	PH left inferior	TP	0.5
pHPT	Right inferior, anterosuperior mediastinum	PA right inferior, PA anterosuperior mediastinum	TP (2x)	0.6, 0.11
pHPT	Right inferior, left inferior	PA right inferior	TP (right), FP (left)	1.0
pHPT	Right inferior	PA right inferior	TP	0.28
pHPT	Right inferior	PA right inferior	TP	1.27
pHPT	Left inferior	PA left inferior	TP	0.65
pHPT	Right inferior	PA right inferior	TP	4.0
pHPT	Right inferior	PA right inferior	TP	1.5
pHPT	Left inferior	PA left inferior	TP	0.5
pHPT	Left superior	PA left superior	TP	0.01
pHPT	Right inferior	PA right inferior	TP	2.37
pHPT	Mid-lower mediastinum	PA mid-lower mediastinum	TP	4.34
pHPT	Left inferior	PA left inferior	TP	2.38
pHPT	Left inferior	PA left inferior (intrathyroidal)	TP	1.38
pHPT	Left inferior	PA left inferior	TP	0.65
pHPT	Right inferior	PA right inferior	TP	0.3
pHPT	Right inferior	PA right inferior	TP	0.52
pHPT	Posterosuperior mediastinum	PA posterosuperior mediastinum	TP	4.41
pHPT	Right superior	PA right superior	TP	3.84
pHPT	Right inferior	PA right inferior	TP	0.81
pHPT	Right inferior	PA right inferior	TP	2.9
pHPT	Left inferior	PA left inferior	TP	0.5
pHPT	Left inferior	PA left inferior	TP	0.36
pHPT	Left inferior	PA left inferior	TP	0.29
pHPT	Right inferior	PA right inferior	TP	0.81
pHPT	Right inferior	PA right inferior	TP	0.55
pHPT	Right inferior	PA right inferior	TP	0.72
pHPT	Left inferior	PA left inferior	TP	1.08
pHPT	Left inferior	PA left inferior	TP	0.09
pHPT	Left inferior	PH left inferior	TP	0.17
pHPT	None	PA left inferior	FN	0.3
pHPT	Right inferior	PA right inferior, PA left superior	TP (right), FN (left)	0.36, 0.29

pHPT, primary hyperparathyroidism; sHPT, secondary hyperparathyroidism; PA, parathyroid adenoma; PH, parathyroid hyperplasia; TP, true positive; FN, false negative; FP, false positive (i.e., thyroid nodule found by histopathology in this patient).

ence of the surgical diagnosis on the pathologist's diagnosis. When a subtotal parathyroidectomy is performed, more hyperplasia is diagnosed. When a focused operation is performed with removal of a single gland, it is likely to be called an adenoma. The importance of mild hyperplasia and the best way of diagnosing this condition have yet to be determined (47).

First reported in 1963 by Wermer (48), MEN syndromes consist of rare, autosomal dominant mutations in genes regulating cell growth. Current classification recognizes MEN 1 and MEN 2, with subcategories MEN 2A (Sipple syndrome) and MEN 2B. MEN 1 is defined by hyperfunctioning tumors of all four parathyroid glands, pancreatic islets (including gastrinoma, insulinoma, glucagonoma, vasoactive intestinal peptide tumor [VIPoma], and pancreatic polypeptide–producing tumor [PPoma]), and the anterior pituitary gland (including prolactinoma, somatotropinoma, corticotropinoma, or nonfunctioning tumors). Other associated tumors include lipomas, angiofibromas, or those located in the adrenal gland cortex. At the time of operation, multiple gland involvement of the parathyroids is typical, although it may be quite asymmetric. Single adenomas and parathyroid cancer have also been described in the setting of MEN 1 (49, 50). One patient in our study with MEN 1 had an adenoma posterior to the superior pole of the right thyroid lobe and a hyperplastic parathyroid gland posterior to the inferior pole of the contralateral thyroid lobe.

It is known that tracer accumulation and retention is not limited to the presence of a parathyroid adenoma or hyperplasia. Less than 1% of parathyroid carcinomas are the culprit of positive imaging findings, and in some cases a thyroid nodule is the reason for false-positive findings, as was the case for one patient of Group 2 in our study (51).

PET and PET-CT with C-11 methionine is an alternative imaging technique to identify hyperfunctioning parathyroid tissues in primary, secondary and recurrent or persistent hyperparathyroidism. PET offers advantages over SPECT; in particular, PET has superior spatial resolution. The high sensitivity of C-11 methionine may also be explained by characteristics in the intermediary metabolism such as transmembrane amino acid transport, protein synthesis and methionine donor transmethylation. Although the number of cases studied to date with C-11 methionine PET is still small, its efficacy in localizing hyperfunctioning glands in hyperparathyroidism appears to be superior to that of Tc-99m sestamibi (52–55).

The sensitivity in the presented cases of eight patients (Group 3, sensitivity per patient: 100%, sensitivity per adenoma: 88.9%) is comparable to those previously published (56). Rubello et al. (57) stated that size may not be the best determinant of dysfunction of parathyroid glands and concluded that C-11 methionine PET may provide additional information in the evaluation of patients with negative or equivocal findings on parathyroid scans.

The most significant limitation of our study was the small number of patients receiving C-11 methionine PET or PET-CT. Further clinical trials with larger patient populations for a reliable statistical analysis are needed to prove the superiority of C-11 methionine PET or PET-CT, particularly in cases of negative Tc-99m sestamibi SPECT examinations.

In conclusion, for the detection of parathyroid adenomas, SPECT is clearly superior to planar imaging. SPECT-CT has identical sensitivity compared to SPECT alone, but it provides additional topographic information that is relevant for subsequent surgery, particularly in cases of ectopic glands. Thus, parathyroid SPECT-CT is highly accurate for the localization of parathyroid adenomas. The sensitivity of PET appears to be even higher compared to that of SPECT, although the number of patients in this study is too small for statistical analysis. In the case of negative scintigraphic findings and proven hyperparathyroidism, additional C-11 methionine PET or PET-CT should be performed (Fig. 6).

Conflict of interest disclosure

The authors declared no conflicts of interest.

References

1. Clark OH, Siperstein AE. The hypercalcemic syndrome. In: Friesen SR and Thompson NW, ed. Surgical endocrinology clinical syndromes. 2nd ed. Philadelphia: Lippincott, 1990; 311–339.
2. Heath H, Hodgson SF, Kennedy MA. Primary hyperparathyroidism: incidence, morbidity, and potential economic impact in a community. N Engl J Med 1980; 302:189–193.
3. Rubello D, Gross MD, Mariani G, Al-Nahhas A. Scintigraphic techniques in primary hyperparathyroidism: from preoperative localisation to intra-operative imaging. Eur J Nucl Med Mol Imaging 2007; 34:926–933.
4. Kinder BK, Stewart AF. Hypercalcemia. Curr Probl Surg 2002; 39:349–448.
5. Loftus KA, Anderson S, Mulloy AL, Terris DJ. Value of sestamibi scans in tertiary hyperparathyroidism. Laryngoscope 2007; 117:2135–2138.
6. Marx SJ. Hyperparathyroid and hypoparathyroid disorders. N Engl J Med 2000; 343:1863–1875.
7. Metz D, Jensen R, Allen B, et al. Multiple endocrine neoplasia type I: clinical features and management. In: Bilezikian J, Levine M, Marcus R, eds. The parathyroids. 1st ed. New York: Raven Press, 1994; 591–647.
8. Kraimps JL, Denizot A, Carnaille B, et al. Primary hyperparathyroidism in multiple endocrine neoplasia type IIa: retrospective French multicentric study. World J Surg 1996; 20:808–812; discussion 812–813.
9. Feliciano DV. Parathyroid pathology in an intrathyroidal position. Am J Surg 1992; 164:496–500.
10. Krubsack AJ, Wilson SD, Lawson TL, et al. Prospective comparison of radionuclide, computed tomographic, sonographic, and magnetic resonance localization of parathyroid tumors. Surgery 1989; 106:639–644; discussion 644–646.
11. Caixas A, Berna L, Hernandez A, et al. Efficacy of preoperative diagnostic imaging localization of Tc-99m sestamibi scintigraphy in hyperparathyroidism. Surgery 1997; 121:535–541.
12. Kaczirek K, Prager G, Kienast O, et al. Combined transmission and Tc-99m sestamibi emission tomography for localization of mediastinal parathyroid glands. Nuklearmedizin 2003; 42:220–223.
13. Massaro A, Cittadin S, Rampin L, et al. Accurate planning of minimally invasive surgery of parathyroid adenomas by means of [(99m)Tc]MIBI SPECT. Minerva Endocrinol 2007; 32:9–16.
14. Lorberboym M, Ezri T, Schachter PP. Preoperative technetium Tc-99m sestamibi SPECT imaging in the management of primary hyperparathyroidism in patients with concomitant multinodular goiter. Arch Surg 2005; 140:656–660.
15. Rubello D, Pelizzo MR, Boni G, et al. Radioguided surgery of primary hyperparathyroidism using the low-dose 99mTc-sestamibi protocol: multiinstitutional experience from the Italian Study Group on Radioguided Surgery and Immunoscintigraphy. J Nucl Med 2005; 46:220–226.
16. Rubello D, Pelizzo MR, Gross MD, Fig LM, Shapiro B, Mariani G. Controversies on minimally invasive procedures for radioguided surgery of parathyroid tumours. Minerva Endocrinol 2004; 29:189–193.

17. Van der Wall H, Carmalt H, Fogelman I. Tc-99m sestamibi and minimally invasive radioguided surgery for primary hyperparathyroidism. J Nucl Med 2005; 46:198–199.
18. Gotthardt M, Lohmann B, Behr TM, et al. Clinical value of parathyroid scintigraphy with technetium-99m methoxyisobutylisonitrile: discrepancies in clinical data and a systematic metaanalysis of the literature. World J Surg 2004; 28:100–107.
19. Neumann DR, Esselstyn CB Jr, Go RT, Wong CO, Rice TW, Obuchowski NA. Comparison of double-phase Tc-99m sestamibi with I-123 / Tc-99m sestamibi subtraction SPECT in hyperparathyroidism. AJR Am J Roentgenol 1997; 169:1671–1674.
20. Neumann DR, Esselstyn CB Jr, Madera A, Wong CO, Lieber M. Parathyroid detection in secondary hyperparathyroidism with I-123/Tc-99m sestamibi subtraction single photon emission computed tomography. J Clin Endocrinol Metab 1998; 83:3867–3871.
21. Rubella D, Pelizzo MR, Casara D. Nuclear medicine and minimally invasive surgery of parathyroid adenomas: a fair marriage. Eur J Nucl Med Mol Imaging 2003; 30:189–192.
22. Sackett WR, Barraclough B, Reeve TS, Delbridge LW. Worldwide trends in the surgical treatment of primary hyperparathyroidism in the era of minimally invasive parathyroidectomy. Arch Surg 2002; 137:1055–1059.
23. McBiles M, Lambert AT, Cote MG, Kim SY. Sestamibi parathyroid imaging. Semin Nucl Med 1995; 25:221–234.
24. Chen CC, Holder LE, Scovill WA, Tehan AM, Gann DS. Comparison of parathyroid imaging with technetium-99m-pertechnetate/sestamibi subtraction, double-phase technetium-99m-sestamibi and technetium-99m-sestamibi SPECT. J Nucl Med 1997; 38:834–839.
25. Billotey C, Sarfati E, Aurengo A, et al. Advantages of SPECT in technetium-99m-sestamibi parathyroid scintigraphy. J Nucl Med 1996; 37:1773–1778.
26. Perez-Monte JE, Brown ML, Shah AN, et al. Parathyroid adenomas: accurate detection and localization with Tc-99m sestamibi SPECT. Radiology 1996; 201:85–91.
27. Sfakianakis GN, Irvin GL 3rd, Foss J, et al. Efficient parathyroidectomy guided by SPECT-MIBI and hormonal measurements. J Nucl Med 1996; 37:798–804.
28. Moka D, Voth E, Dietlein M, Larena-Avellaneda A, Schicha H. Technetium 99m-MIBI-SPECT: a highly sensitive diagnostic tool for localization of parathyroid adenomas. Surgery 2000; 128:29–35.
29. Lorberboym M, Minski I, Macadziob S, Nikolov G, Schachter P. Incremental diagnostic value of preoperative 99mTc-MIBI SPECT in patients with a parathyroid adenoma. J Nucl Med 2003; 44:904–908.
30. Krausz Y, Bettman L, Guralnik L, et al. Technetium-99m-MIBI SPECT-CT in primary hyperparathyroidism. World J Surg 2006; 30:76–83.
31. Takebayashi S, Hidai H, Chiba T, Takagi Y, Nagatani Y, Matsubara S. Hyperfunctional parathyroid glands with 99mTc-MIBI scan: semiquantitative analysis correlated with histologic findings. J Nucl Med 1999; 40:1792–1797.
32. Melloul M, Paz A, Koren R, Cytron S, Feinmesser R, Gal R. Tc-99m MIBI scintigraphy of parathyroid adenomas and its relation to tumour size and oxyphil cell abundance. Eur J Nucl Med 2001; 28:209–213.
33. Ishibashi M, Nishida H, Okuda S, Suekane S, Hayabuchi N. Localization of parathyroid glands in hemodialysis patients using Tc-99m sestamibi imaging. Nephron 1998; 78:48–53.
34. Nishida H, Ishibashi M, Hiromatsu Y, et al. Comparison of histological findings and parathyroid scintigraphy in hemodialysis patients with secondary hyperparathyroid glands. Endocr J 2005; 52:223–228.
35. Mariani G, Gulec SA, Rubello D, et al. Preoperative localization and radioguided parathyroid surgery. J Nucl Med 2003; 44:1443–1458.
36. Nudelman IL, Deutsch AA, Reiss R. Primary hyperparathyroidism due to mediastinal parathyroid adenoma. Int Surg 1987; 72:104–108.
37. Casara D, Rubello D, Cauzzo C, et al. Tc-99m MIBI radio-guided minimally invasive parathyroidectomy: experience with patients with normal thyroids and nodular goiters. Thyroid 2002; 12:53–61.
38. Wang CA. Parathyroid re-exploration: a clinical and pathological study of 112 cases. Ann Surg 1977; 186:140–145.
39. Wang CA. Hyperfunctioning intrathyroid parathyroid gland: a potential cause of failure in parathyroid surgery. J R Soc Med 1981; 74:49–52.
40. Wang CA. The anatomic basis of parathyroid surgery. Ann Surg 1976; 183:271–275.
41. Thompson NW, Eckhauser FE, Harness JK. The anatomy of primary hyperparathyroidism. Surgery 1982; 92:814–821.
42. Kaplan EL, Yashiro T, Salti G. Primary hyperparathyroidism in the 1990s. Choice of surgical procedures for this disease. Ann Surg1992; 215:300–317.
43. Prasad B, Fleming RM. Intrathyroidal parathyroid adenoma. Clin Nucl Med 2005; 30:467–469.
44. Grimelius L, Johansson H. Pathology of parathyroid tumors. Semin Surg Oncol 1997; 13:142–154.
45. Shan L, Nakamura M, Nakamura Y, et al. Comparative analysis of clonality and pathology in primary and secondary hyperparathyroidism. Virchows Arch 1997; 430:247–251.
46. Larian B, Alavi S, Roesler J, et al. The role of hyperplasia in multiple parathyroid adenomas. Head Neck 2001; 23:134–139.
47. Lee NC, Norton JA. Multiple-gland disease in primary hyperparathyroidism: a function of operative approach? Arch Surg 2002; 137:896–899; discussion 899–900.
48. Wermer P. Endocrine adenomatosis and peptic ulcer in a large kindred. Inherited multiple tumors and mosaic pleiotropism in man. Am J Med 1963; 35:205–212.
49. Marx SJ, Menczel J, Campbel G, Aurbach GD, Spiegel AM, Norton JA. Heterogeneous size of the parathyroid glands in familial multiple endocrine neoplasia type 1. Clin Endocrinol 1991; 35:521–526.
50. Hellman P, Skogseid B, Juhlin C, Akerstrom G and. Rastad J. Findings and long-term result of parathyroid surgery in multiple endocrine neoplasia type 1. World J Surg 1992; 16:718–723.
51. Krausz Y, Lebensart PD, Klein M, et al. Preoperative localization of parathyroid adenoma in patients with concomitant thyroid nodular disease. World J Surg 2000; 24:1573–1578.
52. Cook GJ, Wong JC, Smellie WJ, Young AE, Maisey MN, Fogelman I. C-11 methionine positron emission tomography for patients with persistent or recurrent hyperparathyroidism after surgery. Eur J Endocrinol 1998; 139:195–197.
53. Sundin A, Johansson C, Hellman P, et al. PET and parathyroid L-[carbon-11]methionine accumulation in hyperparathyroidism. J Nucl Med 1996; 37:1766–1770.
54. Hellman P, Ahlstrom H, Bergstrom M, et al. Positron emission tomography with C-11 methionine in hyperparathyroidism. Surgery 1994; 116:974–981.
55. Otto D, Boerner AR, Hofmann M, et al. Preoperative localisation of hyperfunctional parathyroid tissue with C-11 methionine PET. Eur J Nucl Med Mol Imaging 2004; 31:1405–1412.
56. Beggs AD, Hain SF. Localization of parathyroid adenomas using C-11 methionine positron emission tomography. Nucl Med Commun 2005; 26:133–136.
57. Rubello D, Fanti S, Nanni C, et al. C-11 methionine PET-CT in Tc-99m sestamibi-negative hyperparathyroidism in patients with renal failure on chronic haemodialysis. Eur J Nucl Med Mol Imaging 2006; 33:453–459.